Ultrasonics 138 (2024) 107216

Contents lists available at ScienceDirect

Ultrasonics

journal homepage: www.elsevier.com/locate/ultras

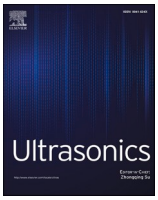

Temperature dependence of acoustic parameters in pure and blended edible oils: Implications for characterization and authentication

A. Jiménez [a], M. Rufo [a], J.M. Paniagua [a], A. González-Mohino [b,*], L.S. Olegario [b]

[a] Department of Applied Physics, Research Institute of Meat and Meat Products, School of Technology, Universidad de Extremadura, Avenida de la Universidad s/n, 10003 Cáceres, Spain
[b] Department of Food Technology, Research Institute of Meat and Meat Products, Universidad de Extremadura, Avenida de la Universidad s/n, 10003 Cáceres, Spain

ARTICLE INFO

Keywords:
Ultrasonic pulse velocity
Ultrasonic global loss
FFT
Edible oils
Temperature
Adulteration
Fat acids

ABSTRACT

This research investigates the temperature-dependent variation of diverse acoustic parameters in samples of edible oils. It further supplements previous studies on the effectiveness of non-destructive ultrasonic inspection in the authentication of edible oils. The oils under examination consist of pure samples of olive, sunflower, and corn oils, as well as variable mixtures ranging from 20 % to 80 % of the more expensive one (olive oil) with the other two, simulating a hypothetical adulteration scenario. The studied acoustic parameters are related to the velocity, attenuation, and frequency components present in 2.25 MHz ultrasonic waves propagating through the oil samples within a temperature range of 24 °C to 34 °C. The results confirm the suitability of non-destructive ultrasonic inspection in evaluating and detecting the adulteration of olive oil with economically inferior oils such as sunflower and corn. Additionally, this study provides added value by laying the groundwork for a non-destructive and innovative determination of the fatty acid profile of an edible oil based on the evolution of the aforementioned ultrasonic parameters with temperature. The findings hold potential for enhancing the authenticity assessment and quality control of edible oils in the food industry.

1. Introduction

Sunflower and corn oils are vegetable oils obtained from the seeds of their respective plants, whereas olive oil is a vegetable oil derived from the fruit (endosperm) of the olive tree. All three are edible oils and, similar to animal-derived oils, they consist of mixtures of triglycerides, comprising approximately 96 % of their composition [1]. Triglycerides consist of three molecules of fatty acids bound to one molecule of glycerol. Additionally, other minor components are also present, such as monoglycerides and diglycerides (where each glycerine molecule combines with one or two molecules of fatty acids, respectively), free fatty acids (responsible for acidity), vitamins, sterols, pigments (chlorophyll, carotenoids, etc.), and other liposoluble substances (tocopherols, etc.) [2].

The diverse composition and favorable fatty acid profile of edible vegetable oils make them an integral component of a balanced diet [3,4]. The issue of adulteration of edible vegetable oils, such as olive oil, with cheaper oils is of significant concern due to its economic, health, and consumer fraud implications. Adulterated oils can compromise the quality, authenticity, and nutritional value of the product, leading to potential health risks and consumer deception. Detecting and preventing such adulteration is crucial to safeguard consumer trust and ensure the integrity of the edible oil market [5,6].

The evaluation of the quality of olive oil is carried out using traditional analysis techniques, either physical–chemical, microbiological or sensory. This, on the one hand, supposes the destruction of the product, and, on the other hand, generates chemical residues that must be treated later, with the consequent problem of waste generation. In addition, the time needed for a complete analysis is high and carries with it an economic cost, to which the high price of the samples of this type of products is added [7,8].

The application of non-destructive analysis techniques, particularly ultrasound, holds a pivotal role in detecting adulteration in edible vegetable oils. Ultrasound-based methods offer several advantages, including swift analysis, non-invasiveness, and the capability to assess multiple parameters concurrently. Several studies have substantiated the efficacy of ultrasound in identifying adulterants, thereby ensuring the authenticity and quality of edible vegetable oils. The adoption of ultrasound-based techniques can significantly improve the efficiency and precision of detecting oil adulteration, thus safeguarding consumer

* Corresponding author at: Universidad de Extremadura, IPROCAR, Avda. de la Universidad s/n, 10003 Cáceres, Spain.
E-mail address: albertogj@unex.es (A. González-Mohino).

https://doi.org/10.1016/j.ultras.2023.107216
Received 2 August 2023; Received in revised form 10 November 2023; Accepted 4 December 2023
Available online 5 December 2023

health and upholding the integrity of the product [1,9–16].

This research is part of the aforementioned line of study. Its primary objective is to ultrasonically characterize three of the most consumed edible oil varieties (olive, sunflower, and corn), as well as various blends of the more expensive oil (olive) with the other two, simulating potential adulteration scenarios. This characterization is carried out by not only using the velocity of ultrasonic wave propagation and its global loss, parameters commonly employed in this field [1,11,12,14,17–19], but also by introducing other more innovative parameters related to the frequency components present in their transmission through the samples [15]. In this context, this work complements other previous research by the authors carried out with the same samples and methods [16]. Additionally, the characterization is complemented by studying the evolution of all these parameters with temperature, given its proven effect on the acoustic parameters of various materials [20,21]. Concurrently, we apply this characterization for sample authentication. As an added value, this work also contributes to establishing some groundwork for estimating the predominant triglycerides (fatty acid profile) present in the edible oils through non-destructive ultrasonic inspection.

2. Material and methods

2.1. Samples

Three types of edible oils from the 'Coosol' brand (Jaén, Spain) were purchased: olive oil, sunflower oil, and corn oil. Six one-liter bottles of each oil type were acquired, resulting in a total of eighteen bottles (6 bottles per type). To create a diverse set of samples, eleven different batches were prepared, each in triplicate, amounting to a total of 33 samples. Out of these batches, three were composed of pure samples of each type of oil. The remaining eight batches were formed by blending different proportions of the three main samples. In Table 1, the composition of the eleven prepared batches is indicated. It is important to note that, in order to achieve maximum heterogeneity in the bottles, they were purchased from six different supermarkets, ensuring that bottles of the same type of oil did not belong to the same factory batches, a fact that was verified. For the same reason, the six one-litre bottles of each oil type were never mixed together to obtain three "unique" oil types from which to prepare the described eleven batches. Instead, these batches were created by randomly selecting bottles from their respective sources. For instance, if we denote O1…O6 as the six bottles of olive oil, S1…S6 as those of sunflower oil, and C1…C6 as those of corn oil, the three replicates of the OC (40–60) sample, for example, could have been prepared from bottles O3 + C6, O1 + C1, and O4 + C6. It should be noted that no control was exercised over the constituent bottles of each of the 33 samples in this regard.

2.2. Ultrasound inspection

The ultrasound inspection was conducted following a procedure similar to previous works [15,16]. A volume of 150 ml was taken from each of the 33 prepared samples and introduced into a Nessler tube with a capacity of 200 ml. Subsequently, each aliquot was heated to 34 °C in a thermostatic bath (JP SELECTA, Spain). Ultrasonic tests were conducted at 2 °C intervals, starting from this temperature and cooling down to room temperature until reaching a final temperature of 24 °C. Consequently, a total of 198 ultrasonic tests were performed using the pulse-echo (PE) immersion technique to inspect the samples. For this purpose, the Olympus Model V305-SU piezoelectric transducer with a nominal frequency of 2.25 MHz was selected (main characteristics described in Table 2). During the inspection, the transducer was positioned at the top of the Nessler tube, submerged to a depth of approximately 1.5 cm in the oil. To accomplish this, the transducer was integrated onto a bespoke metal structure that ensured, on one hand, its precise alignment with the bottom of the tube and, on the other hand, its isolation from potential signals originating from the glass or the metal structure itself through elastic rubber fastenings. The distance between the transducer's surface and the bottom of the Nessler tube, which acted as a reflecting mirror for the ultrasonic waves, was measured with a precision caliper with an accuracy of ± 0.01 mm. This distance was 158.00 mm. This distance ensured that the measurements were conducted in the far field (Fraunhofer region) since, in the pulse-echo mode, the ultrasonic waves travel a minimum distance from emission to reception, amounting to 158.00x2 = 316.00 mm. This distance is substantially greater than the length of the near field (Fresnel region) specified in Table 2. The deliberate selection of the far field region was critical to prevent wave interference phenomena from affecting the evaluation of parameters linked to the attenuation and frequency of the received signal. By working in the far field, any potential interference issues were mitigated, ensuring the accurate assessment of these parameters [22].

The ultrasonic measurements were carried out using the Olympus-NDT Model 5077PR Pulser-Receiver, responsible for emitting and receiving signals from the piezoelectric transducer. This equipment was connected to a KEYSIGHT InfiniiVision DSO-X 3032A oscilloscope, which was utilized to register and save the A-scans with 10,000 points in csv format. The experimental setup used for these measurements is illustrated in Fig. 1. During the ultrasonic tests, a total of 3 A-scans were recorded from each of the 198 tests performed. Each A-scan was obtained with a different time interval (*TI*) on the oscilloscope, with the specific objectives as follows: (i) $TI = 2000$ μs: This interval captured the trigger pulse and the first seven full echoes. (ii) $TI = 500$ μs: This interval encompassed the first two full echoes. (iii) $TI = 250$ μs: This interval included only the first full echo. In total, the study encompassed the treatment and analysis of 594 A-scans. As an example, Supplementary Material 1 (SM1) exhibits the three characteristic A-scans corresponding to one of the inspected aliquots, providing valuable insights into the signal characteristics at different time intervals. In all three types of A-scan, less intense signals can be observed, which originate from successive reflections on the front and back surfaces of the bottom of the Nessler tube, as well as on the lateral faces of the tube itself. To study the influence exerted by these successive reflections on the signal of each echo, Supplementary Material 2 (SM2) shows a zoom of the A-scan region where the reception of echo 1 begins. Given that the glass thickness of the Nessler tube bottom (distance from the front to the back surfaces) is 3.54 mm, and considering a sound propagation velocity in the glass, denoted as v_g, within the range [4000–5000] m/s [23], the first arrival at the transducer from the wavefront that has experienced a previous transmission-reflection at the tube bottom would occur after a time $t_g = (2 \cdot 3.54 \cdot 10^{-3}) / v_g$. In other words, this time interval ranges from 1.42 μs (for 5000 m/s) to 1.77 μs (for 4000 m/s) from the arrival of the wavefront that solely reflects at the front face of the tube bottom. It should be noted that this time interval is greater than the waveform duration at −20 dB level shown in Table 2, that is, the oscillation amplitude of the transducer would decrease in that time interval more than ten times assuming that it received, which does not happen, a single pulse. For the wavefront resulting from a double reflection-transmission process at the

Table 1
Composition of prepared sample batches.

Batch number	Olive oil (%)	Sunflower oil (%)	Corn oil (%)
i	100	0	0
ii	0	100	0
iii	0	0	100
iv	80	20	0
v	60	40	0
vi	40	60	0
vii	20	80	0
viii	80	0	20
ix	60	0	40
x	40	0	60
xi	20	0	80

Table 2
Main transducer characteristics.

Model	Diameter (cm)	Frequency (MHz)	Waveform duration (μs)	−6 dB Bandwidth (%)	λ (mm)	N (mm)	φ (°)
Panametrics V305-SU	1.9	2.25	−20 dB level: 1.080 −40 dB level: 2.040	61.9	0.64	140.0	2.37

The ultrasonic propagation velocity $UPV = 1450$ m/s was taken for the calculation of λ, N and φ.
λ: wavelength.
N: near-field length.
φ: beam angle.

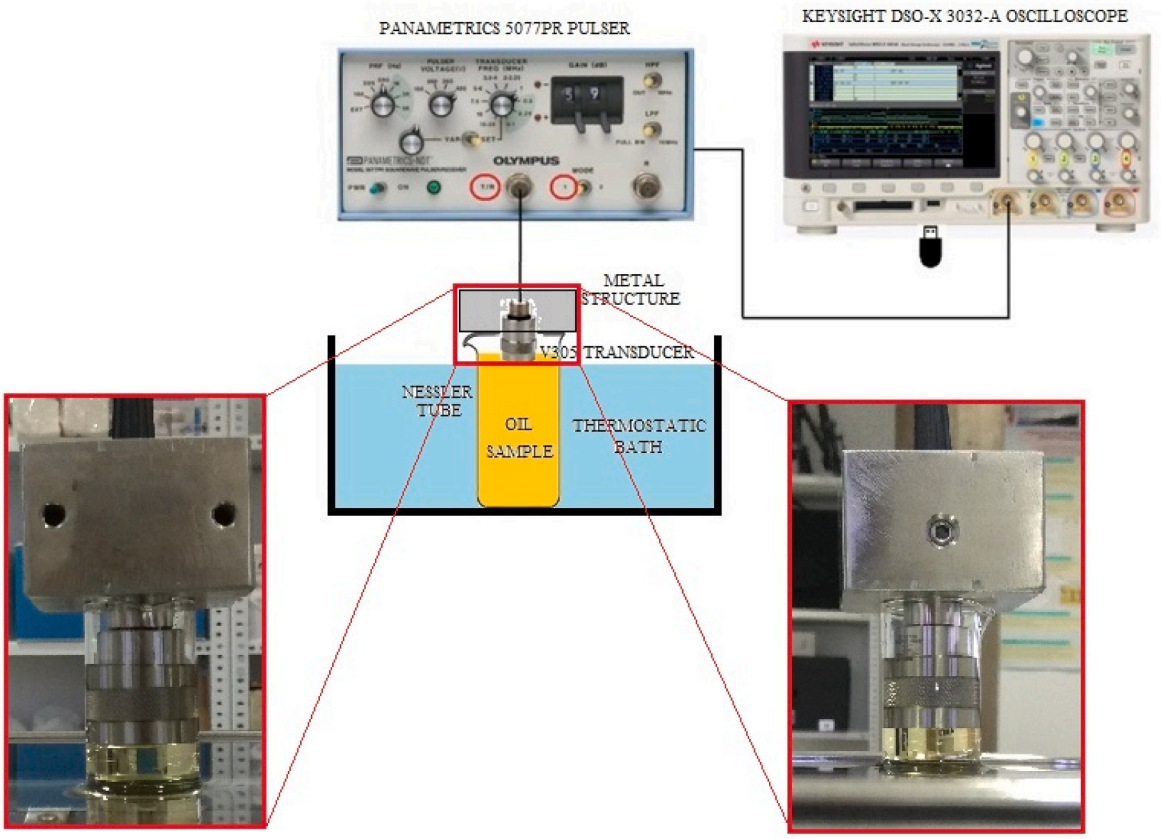

Fig. 1. Block diagram for the experimental ultrasonic measurements.

bottom, it would arrive at twice the indicated time range, and so on. In Figure SM2, the regions of maximum amplitude have been identified where these three initial arrivals are expected, which we will refer to as sub-echoes for clarity in the exposition. As can be observed, all these sub-echoes occur within the temporal interval identified as echo 1. Naturally, the amplitude of each sub-echo decreases as it moves away from the first one. Furthermore, the amplitude of each sub-echo is clearly affected by the preceding sub-echo, but the reverse does not appear to be the case. In other words, the peak-to-peak amplitude of sub-echo 1 does not seem to be altered by sub-echo 2. Thus, it can be assumed that the peak-to-peak amplitude of echo 1 is equivalent to that of the wavefront reaching the transducer after undergoing only a reflection at the front surface of the Nessler tube bottom (sub-echo 1). This deduction can be made identically for each of the seven echoes considered in the study. Furthermore, since the flight time of waves through the oil is significantly higher compared to the flight times in the glass due to reflection-transmission processes of the sub-echoes at the tube bottom, none of the echoes shown in SM1a would be significantly affected by the sub-echoes of immediately preceding echoes. For instance, between echo 2 and echo 1, more than 200 μs elapse, meaning it would be affected by those wavefronts that have undergone more than 130 successive reflection-transmission processes at the Nessler tube bottom, which, if they occur, would have a negligible amplitude.

As stated, the ultrasonic parameters under investigation were as follows: propagation velocity (*UPV*); ultrasonic global loss (*UGL*); and frequency values for which 25 %, 50 %, and 75 % (*FFT25*, *FFT50*, and *FFT75*, respectively) of the entire frequency spectrum obtained in the FFT are received.

2.2.1. Some previous particularities

The methodologies employed to calculate the previously mentioned ultrasonic parameters are essentially the same as those outlined in prior studies [15,16,24,25]. However, for clarity and briefness, only the aspects that differ from the procedures mentioned in those works have been emphasized in the current study. The underlying calculation principles and techniques have been retained, ensuring consistency and comparability with the prior research.

Regarding the calculation of UPV (propagation velocity), two methods were employed, both utilizing the A-scans with $TI = 2000$ μs: (i) Least squares fit: This method involved performing a least-squares fit to the equation of a straight line, which relates the known distance covered by the ultrasonic signal to the corresponding time of flight for

each of the seven echoes, utilizing for that the time of arrival at the maximum amplitude. Supplementary Material 3 (SM3) provides an example of the aforementioned information. The slope of this fit provided the propagation velocity, denoted as UPV_{lr} [15]. (ii) Cepstrum method: The calculation is based on the FFT of the A-scan. By way of example, Supplementary Material 4 (SM4) showcases the FFT generated from the A-scan of Figure SM1a. The influence of a periodic excitation (here multiple echoes) shows up as maxima in the spectrum at multiples of the fundamental frequency, and thus as superpositions of the fundamental spectrum of the probe with an undulation in the form of equidistant maxima in the spectrum. The time of flight between the echoes generated by successive reflections between the bottom of the Nessler tube and the surface of the transducer is obtained from the distances of the maxima. By means of the so-called cepstrum method, the spectrum can be smoothed and the length of the period determined directly. The cepstrum arises by a FFT of the logarithmized spectrum [26,27]. Algorithmically, the cepstrum C is given by equation (1):

$$C = FFT^{-1}\{\mathrm{LN}[FFT(A-scan)]\} \tag{1}$$

This second FFT directly displays the time (t) elapsed between these excitations (time of flight between two consecutive echoes). By combining this information with the known distance (0.316 m) travelled by the ultrasonic wave between these echoes, the velocity $UPV_{cepstrum}$ could be directly calculated as $UPV_{cepstrum} = 0.316/t$. As an illustrative example, Supplementary Material 5 (SM5) showcases the cepstrum generated from the A-scan of Figure SM1a. Both methods were previously validated in water to ensure their accuracy and reliability. In this particular study, the velocity in distilled water was determined at two different temperatures: 24 °C and 34 °C. The results obtained using the least squares fit method were (1493 ± 3) m/s and (1517 ± 3) m/s, and those obtained through the cepstrum method were (1497.6 ± 2.1) m/s and (1517.3 ± 2.1) m/s. These results are consistent with values reported by previous researchers, such as Del Grosso and Mader, who utilized a high-frequency interferometry method [28]. The associated errors for the determinations of UPV_{lr} and $UPV_{cepstrum}$ were found to be of the order of 0.20 % and 0.15 %, respectively. These relatively small errors demonstrate the accuracy and reliability of the velocity measurements obtained through these methods.

Regarding ultrasonic global loss, it should be noted beforehand that it is not necessary to consider diffraction effects of ultrasonic waves propagating through the medium, so a priori, it is the viscosity of the oil that is responsible for it. To illustrate this point, one can consider that the largest molecules present in edible oils are triglycerides (composed of one glycerol molecule and three fatty acids), accounting for more than 90 % of the composition of the studied edible oils. The dimensions of these triglyceride molecules are smaller than 1 nm, making them "invisible" to the ultrasonic signal, whose wavelength λ is much larger (specifically 0.64 mm, as reflected in Table 2). Thus, several of these molecules dispersed in a colloidal solution would create particles smaller than 100 nm [29], a dimension that would still be 10,000 times smaller than the employed λ. In this way, the ultrasonic global loss UGL (in neper/m) was calculated using Eq. (2):

$$UGL = \frac{1}{2d}\mathrm{LN}\frac{A_i}{A_j} \tag{2}$$

where A_i and A_j represent the peak-to-peak amplitudes of echoes i and j, respectively, and 2d corresponds to the distance covered by the ultrasound wave between these two echoes. The evaluation of UGL was based on the analysis of seven echoes obtained from the A-scan corresponding to TI = 2000 μs. The calculation of UGL involved plotting $\mathrm{LN}(A_i/A_j)$ against $2d$, and the slope of this plot provided the value of the ultrasonic global loss [16,30]. Supplementary Material 6 (SM6) provides an example of the aforementioned information. To be precise, the proposed method for calculating UGL slightly deviates from the concept of absolute attenuation, as it involves not only viscosity effects but also those related to reflection and transmission on the rear and, to a lesser extent, lateral faces of the Nessler tube. Therefore, the value obtained for UGL is closely tied to the inspection geometry, and its value can only be compared with those obtained in samples with identical measurement geometry, as is the case with all the samples inspected in this study.

The determination of FFT25, FFT50, and FFT75 is based on the understanding that the ultrasonic frequencies transmitted through the samples do not precisely coincide with the nominal frequencies emitted by the transducer [24,31]. Consequently, it is more meaningful to consider the frequencies that are actually transmitted and appear in the associated FFT for each A-scan. These frequencies in the FFT provide a more accurate representation of the signal characteristics in the frequency domain. However, it is essential to consider a caveat resulting from the Nyquist theorem, which establishes the minimum sampling frequency f' required to correctly study any frequency signal f in the frequency domain, as shown in Eq. (3) [32]:

$$f' \geq 2f \tag{3}$$

For this reason, to calculate the frequency parameters, we selected only the A-scans obtained with TI = 500 μs ($FFT25_{1\text{-}2}$, $FFT50_{1\text{-}2}$, and $FFT75_{1\text{-}2}$) and TI = 250 μs ($FFT25_1$, $FFT50_1$, and $FFT75_1$), with corresponding values of f' being $2{\cdot}10^7$Hz and $4{\cdot}10^7$Hz, respectively. Considering that the central frequency f of the utilized transducer is $2.25{\cdot}10^6$Hz, the aforementioned values of f' unequivocally verify Eq. (3). By way of illustration, Supplementary Material 7 (SM7) displays the Fast Fourier Transforms (FFTs) generated from the A-scans depicted in Figures SM1b and SM1c. Furthermore, for its acquisition, the complete received signal in the corresponding A-scan has not been considered; only the temporal interval of the A-scan containing echoes 1 and 2 (for TI = 500 μs) and echo 1 (for TI = 250 μs). Three observations are pertinent to this matter: (1) Unlike what was observed in the FFTs corresponding to the A-scans of TI = 2000 μs (see SM4) and TI = 500 μs, in the FFT corresponding to TI = 250 μs the characteristic periodic excitation is not apparent, as no echo appears within the considered temporal interval of the A-scan. (2) Despite the transducer having a central frequency of $2.25{\cdot}10^6$Hz and a 6 dB bandwidth of 61.9 %, the obtained FFTs do not exhibit a maximum amplitude at that frequency, but rather at other frequencies that are significantly lower. (3) The normalized amplitude of the FFT corresponding to TI = 500 μs is lower than that of the FFT corresponding to TI = 250 μs, as a consequence of the frequencies present in the former being more attenuated due to considering a greater distance travelled by the wave. Using these FFTs, we constructed cumulative frequency periodograms, displaying the 25th, 50th, and 75th percentiles of the frequencies present in the received signals. In concrete terms, FFT50 would correspond to the minimum frequency value for which 50 % of the total energy would have been received. That is to say, if the 50th percentile of the cumulative frequency were located at x Hz for a particular inspection, this would indicate that 50 % of the received signals would have frequencies lower than x Hz. Identically for FFT25 and FFT75. For illustrative purposes, Supplementary Material 8 (SM8) exhibits the cumulative frequency periodograms generated from the FFTs presented in SM7. One final observation: The values of FFT25, FFT50, and FFT75, corresponding to the A-scan of TI = 500 μs, are slightly lower than those corresponding to TI = 250 μs. This is a result of higher frequencies being more attenuated than lower frequencies in the former, due to considering a greater distance traveled by the wave.

3. Results and discussion

3.1. Ultrasonic velocity results

Fig. 2 illustrates the relationship between the average velocity results obtained from both methods (UPV_{lr} and $UPV_{cepstrum}$) for the inspected samples at different temperatures. As observed, there exists a highly significant linear correlation between the two (R^2 = 0.998). Moreover,

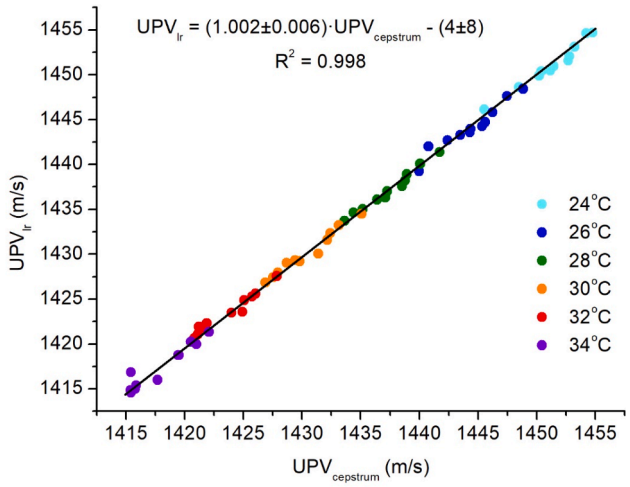

Fig. 2. Evolution of the mean ultrasonic velocity values (UPV_{lr} and $UPV_{cepstrum}$) obtained by both procedures in the samples inspected at different temperatures and linear regression fit between them. The data corresponding to 24 °C and 30 °C have been published in previous works [16].

as expected, the slope value encompasses unity, and the intercept value at the origin is zero. This outcome ensures, first and foremost, the validity of the pursued procedures and further enables the assessment of results based solely on one of the methods, whether *UPV$_{lr}$* or *UPV$_{cepstrum}$*.

Thus, Fig. 3 presents the temperature evolution of *UPV$_{cepstrum}$* values for batches of pure oils and oil mixtures of olive oil with (a) sunflower and (b) corn oils. Firstly, we note that the velocity results are consistent with findings in the literature, which are shown in Table 3.

As observed in all the inspected samples, a highly significant linear relationship exists between both parameters. This behaviour is expected, given the well-known linear relationships between temperature and both density [13] and ultrasonic propagation velocity [14,33] in oil samples. Additionally, for any particular sample, whether pure or mixed, it exhibits a clearly distinct range of velocities at each temperature. It is worth noting that all the samples demonstrate an identical trend of decreasing ultrasonic propagation velocity with increasing temperature. This phenomenon is consistent with findings in existing literature, not only for oils [14] but also for other food matrices such as honey [34,35] and materials in general [36,37]. In principle, this phenomenon could be attributed to the continuous process of triglyceride melting, which is the main component (>95 %) of edible oils, as the temperature rises [38–42]. Consequently, as these triglycerides undergo melting, the velocity decreases. The different composition of triglycerides presents in the three types of pure oils inspected, as well as their abundance percentages, results in distinct regression equations for the linear relationships between velocity and temperature. Similar reasoning could apply to other minor components, such as diglycerides and monoglycerides [43]. As a guide to the aforementioned, Table 4 indicates the proportions of the main components in the studied edible oils and their respective melting temperatures [2,44,45].

For all three varieties of pure oils, the lowest values for both slope and intercept correspond distinctly to olive oil, while the highest values are associated with sunflower oil. In the mixed samples, the regression lines are bounded by those of the corresponding pure oils, distributed more or less proportionally based on the respective percentage of each variety in the mixture. Thus, with an equal percentage of mixture, the slopes and intercepts of the regression lines for the mixture of olive oil with sunflower oil are greater than those with corn oil. Furthermore, it appears that there is a greater overlap in the ultrasonic velocity intervals of the samples at higher inspection temperatures, at least within the temperature range of the study. In fact, the range of velocities considering all the samples is narrower at higher temperatures, as depicted in

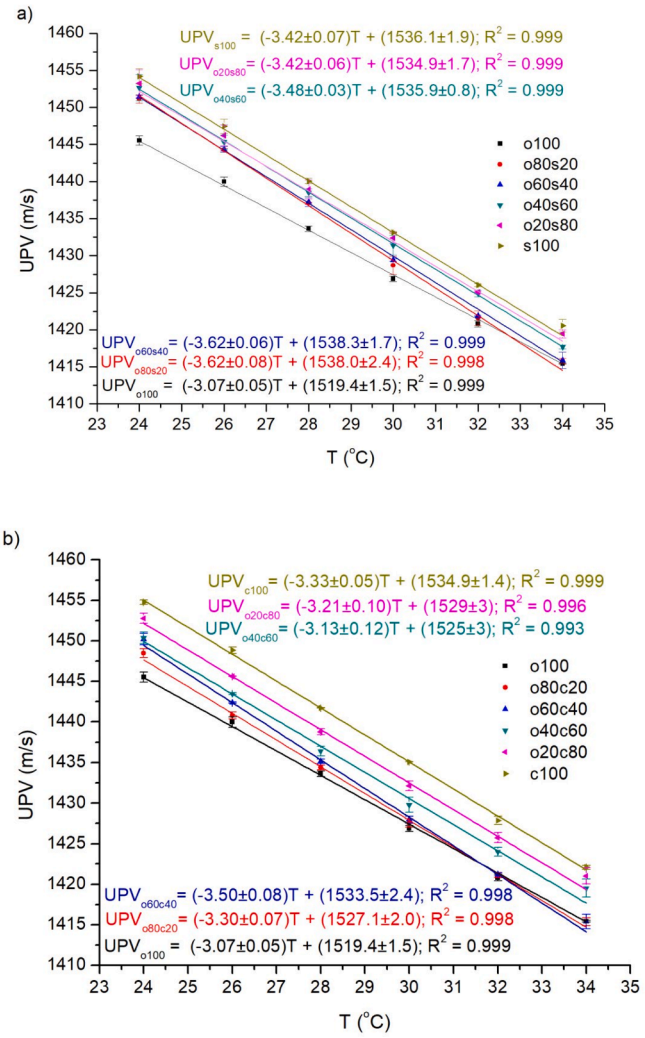

Fig. 3. Evolution with temperature of mean ultrasonic velocity values $UPV_{cepstrum}$ corresponding to the adulteration of pure olive oil with variable percentages of (a) pure sunflower oil and (b) pure corn oil. Error bars indicate standard deviation. The data corresponding to 24 °C and 30 °C have been published in previous works [16].

Fig. 4, where a zoom is applied to the values shown in Fig. 3 for each temperature. Fig. 4 also reveals that, in the mixture of olive oil with corn or sunflower oil, the percentage of the mixture can be discerned in some cases, even considering the error margins. This observation is particularly evident for the case of the mixture with sunflower oil at 24 °C and 28 °C or with corn oil at 32 °C.

3.2. Ultrasonic global loss results

Fig. 5 illustrates the evolution of ultrasonic global loss values (*UGL*) with temperature. Firstly, it is essential to highlight that these values are significantly higher than those obtained in previous studies [15]. This difference is attributed to the higher frequency used in this current research (2.25 MHz) compared to the former (1 MHz). Thus, the ultrasonic global loss obtained with 1 MHz transducers did not exceed the value of 30 dB/m in any of the inspected samples of pure olive, sunflower, or corn oil. As expected, the use of higher frequencies results in a notable increase in ultrasonic global loss, which is precisely what has been observed in this study.

Unlike the behaviour observed with velocity, the ultrasonic global loss does not exhibit a linear relationship with temperature. With the caution warranted by the obtained error margins, it appears that there is

Table 3
Velocity, temperature range and transducer frequency values findings in the literature, for the three types of oils inspected.

Reference	Transducer frequency (MHz)	Olive oil		Sunflower oil		Corn oil	
		Temperature (°C)	Velocity (m/s)	Temperature (°C)	Velocity (m/s)	Temperature (°C)	Velocity (m/s)
Rashed et al. (2018) [17]	1	23	1436.3 ± 0.3	23	1442.3 ± 0.3	23	1441.8 ± 0.3
Yan et al. (2019) [11]	5	[17–36]	[1470–1415]	23.5	1461 ± 1		
Jiménez et al. (2022) [15]	1	[25–29]	[1450–1435]	[25–29]	[1460–1445]	[25–29]	[1462–1452]

Table 4
Melting points and proportion of monoglycerides, diglycerides and triglycerides in olive, sunflower and corn oils.

Composition	Triglyceride composition	Meelting point (°C)	Olive (%)	Sunflower (%)	Corn (%)
Triglycerides	OOO	5.6	[40–59]	5.6	8.16
	POO	18.0	[15–22]	2.1	5.66
	OOL	−2.8	[12–20]	11.3	12.5
	PLO	−1.1	[4–7]	6.7	9.57
	SOO	22.8	[3–7]	1.3	3.24
	POP	35.0	[2–4]	0.3	–
	PLP	27.2	1.2	1.1	–
	POS	37.8	0.3	0.3	2.04
	SOL	6.1	4.2	3.7	6.51
	PLS	30.0	–	1.4	2.47
	PLL	−5.6	–	10.1	9.03
	SLL	1.1	–	7.3	–
	OLL	−6.7	–	26.5	13.52
	LLL	−13.3	–	22.3	12.23
Diglycerides		~20	[1.0–5.5]	2.0	2.8
Monoglycerides		[8–56]	[0.2–0.25]	–	–

O: Oleic cid. P: Palmitic acid. L: linoleic acid. S: Stearic acid. -: Data not reported.

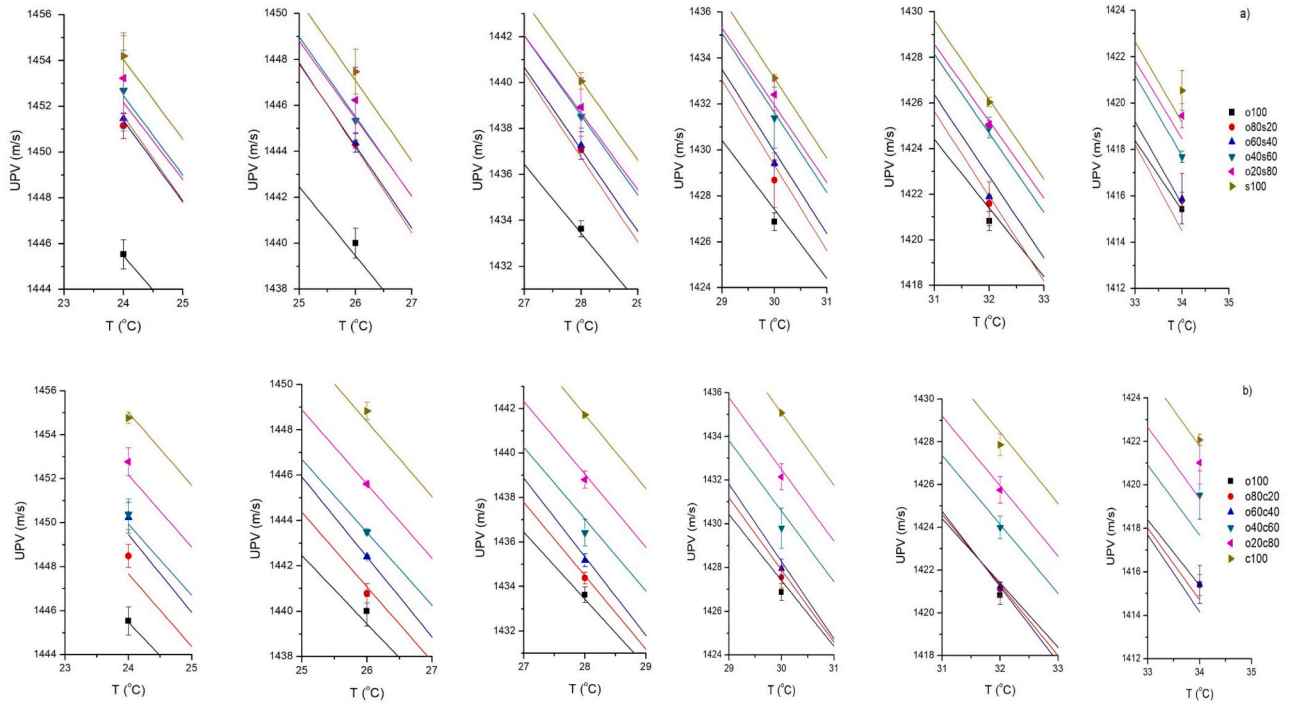

Fig. 4. Zoom of the data shown in Fig. 3 for each temperature.

a maximum value of ultrasonic global loss around 28–30 °C, depending on the inspected sample, which slightly and continuously decreases as the temperature moves away from that range, either above or below. However, this performance is evident across all samples, whether pure or mixed, indicating that it can be attributed to the major triglycerides present in the examined pure and mixed oils. Nonetheless, the absence of a linear relationship between ultrasonic global loss and temperature suggests that the behaviour of triglyceride attenuation with temperature is precisely dependent on the specific triglyceride considered. This is in contrast to velocity, where all triglycerides seemed to behave identically with temperature, i.e., reducing their value as T increases. Although the general behaviour of ultrasonic global loss with temperature is similar

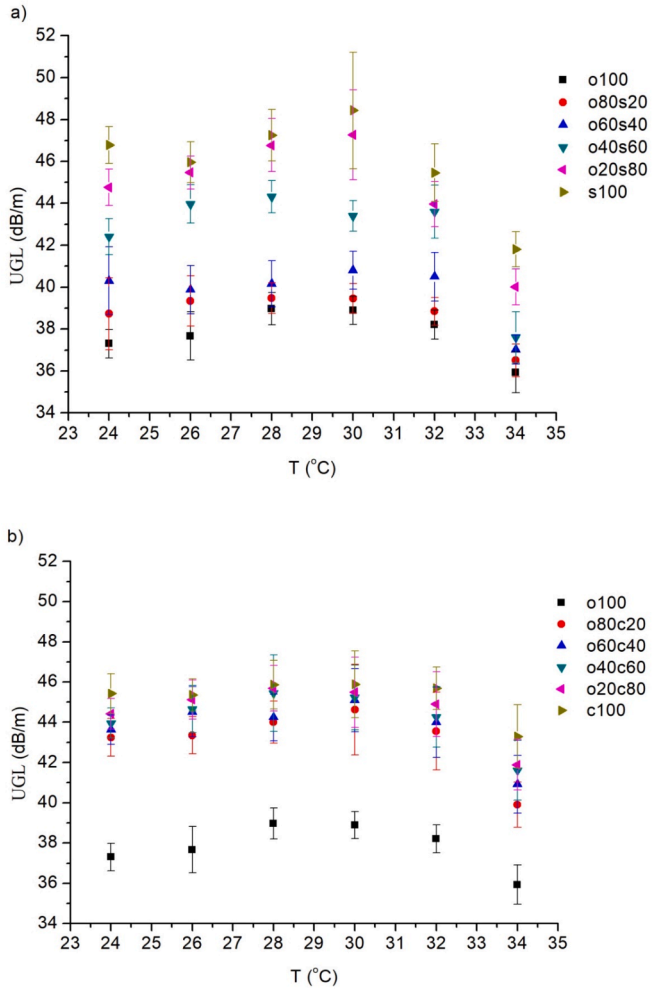

Fig. 5. Evolution with temperature of mean ultrasonic global loss values UGL corresponding to the adulteration of pure olive oil with variable percentages of (a) pure sunflower oil and (b) pure corn oil. Error bars indicate standard deviation. The data corresponding to 24 °C and 30 °C have been published in previous works [16].

across all samples, the ultrasonic global loss values are not directly proportional to the adulteration percentage, particularly evident in the olive-corn adulteration. The distinct composition, not only of each of the studied oil varieties but even within the same variety, depending on the bottle used, appears to account for this variation. While this poses clear disadvantages when drawing conclusions about the observed behaviour, it also offers a significant advantage: ultrasonic global loss would, a priori, be a more sensitive ultrasonic parameter than velocity in distinguishing the major triglycerides present in the samples.

Regarding the pure oils, the lowest ultrasonic global loss values clearly correspond to olive oil. The highest values are associated with sunflower oil, although the error margins do not allow for a clear distinction from corn oil. In the mixed samples, the ultrasonic global loss values are bounded by those of the corresponding pure oils, distributed more or less proportionally based on the percentage presence of each variety in the mixture, particularly noticeable in the olive-sunflower mixture and to a lesser extent in the olive-corn mixture. Once again, due to the obtained error margins, ultrasonic global loss does not allow for a clear separation of most mixed samples from each other. Thus, only pure olive oil is clearly distinguishable from any of its adulterations with corn oil.

3.3. FFT results

In Fig. 6, the relationships between the 25th, 50th, and 75th percentiles of the frequency components obtained from both procedures ($FFT25_1$, $FFT50_1$, $FFT75_1$, $FFT25_{1\text{-}2}$, $FFT50_{1\text{-}2}$, $FFT75_{1\text{-}2}$) are shown for the inspected samples at different temperatures. As observed, the obtained linear relationships are highly significant. This fact also demonstrates the limited influence that the edge effect has when choosing the A-scan considering echoes 1 and 2. This result ensures the validity of the followed procedures and allows for the evaluation of results based on either $FFTxx_1$ or $FFTxx_{1\text{-}2}$. However, it is important to note that while the slope values are close to one in all cases, the y-intercept is clearly negative. Consequently, the values of $FFTxx_{1\text{-}2}$ are slightly lower than the corresponding values of $FFTxx_1$. This result is coherent with what was expected beforehand, as the frequency components present in the signal coming from echoes 1 and 2 should be lower than those from echo 1 only, as in the former case, the waves travel a greater distance and consequently experience more attenuation.

In Fig. 7, the variation of $FFTxx_1$ values with temperature is presented for the batches of pure oils and the adulteration of olive oil with (a) sunflower oil and (b) corn oil. It is worth noting that these values are considerably higher than those obtained in previous works [15]. This difference is a result of the higher frequency utilized in this study (2.25 MHz) in comparison to the previous work (1 MHz).

Unlike the behaviour observed in velocity, none of the studied frequency percentiles exhibit a linear trend with temperature. With the caution required by the obtained error margins, it seems that there are maximum values around 30–32 °C, depending on the specific percentile and sample under consideration, which decrease slightly and continuously as the temperature moves away from that range, either above or below. Additionally, in general, the standard deviation increases with the percentile considered. Consequently, there is significant overlap between the frequency ranges of each sample at each temperature, especially when referring to the 75th percentile. Indeed, it is evident that this behaviour is consistent across all samples, whether they are pure or adulterated. This indicates that the observed phenomenon can be attributed to the predominant triglycerides present in both the pure and mixed oils under inspection. However, the observed lack of a linear relationship between the frequency components of each percentile and temperature suggests that the behaviour of triglyceride attenuation with temperature varies depending on the specific triglyceride considered. This phenomenon, similar to what was observed with ultrasonic global loss, did not occur with velocity, where all triglycerides appeared to

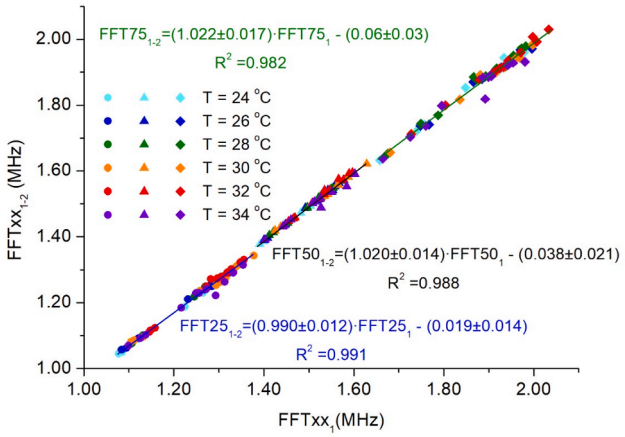

Fig. 6. Evolution of the frequency percentiles 25, 50, and 75 obtained by both procedures ($FFT25_1$, $FFT50_1$, $FFT75_1$, $FFT25_{1\text{-}2}$, $FFT50_{1\text{-}2}$, and $FFT75_{1\text{-}2}$) in the samples inspected at different temperatures and the linear regression fit between them. The data corresponding to 24 °C and 30 °C have been published in previous works [16].

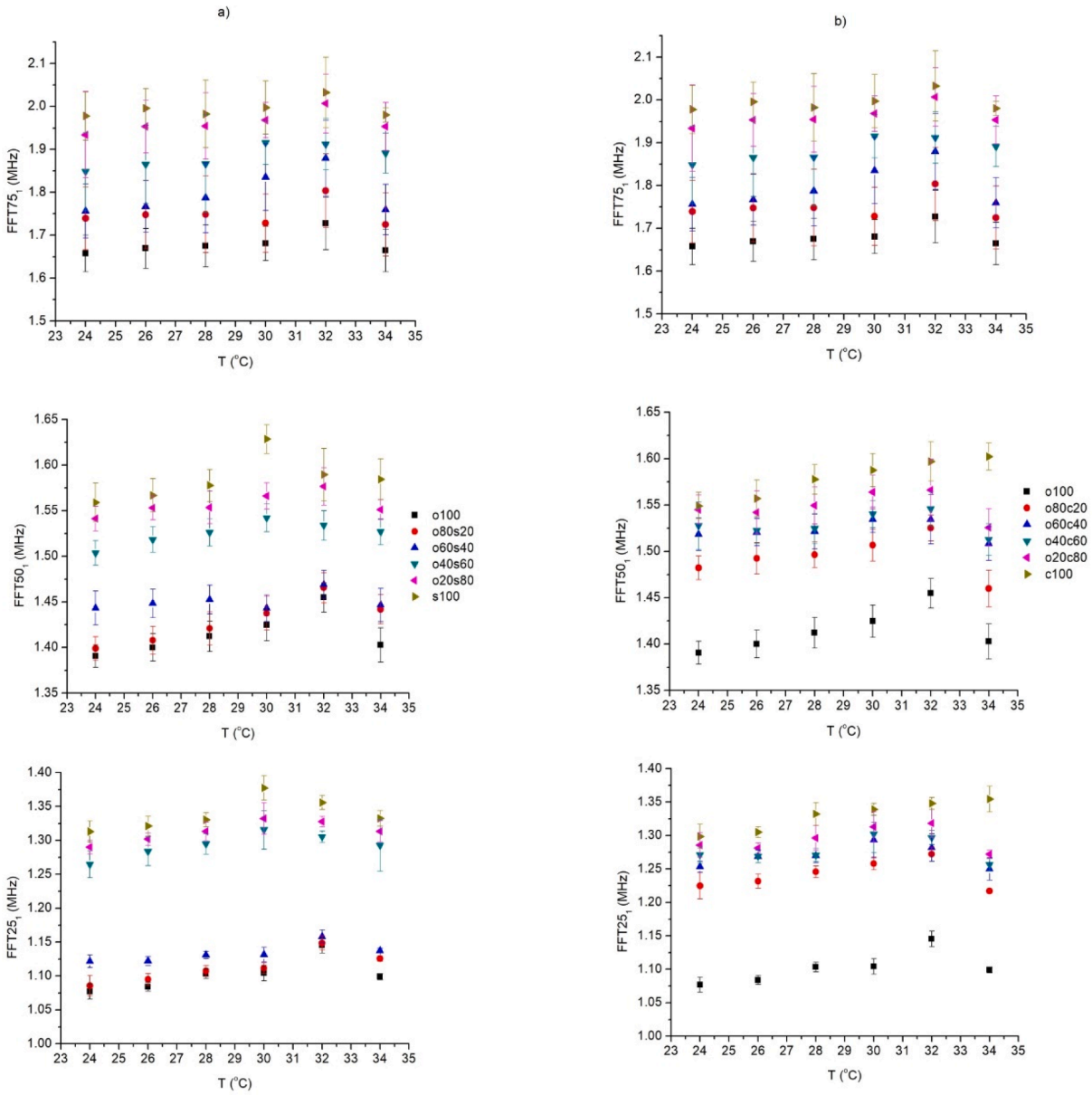

Fig. 7. Evolution with temperature of the frequency percentiles 25, 50, and 75 ($FFT25_1$, $FFT50_1$, and $FFT75_1$) corresponding to the adulteration of pure olive oil with variable percentages of (a) pure sunflower oil and (b) pure corn oil. Error bars indicate standard deviation. The data corresponding to 24 °C and 30 °C have been published in previous works [16].

behave identically with temperature, that is, decreasing in value as the temperature increased. As a result, the distinct composition of each variety of oil studied, and even within the same variety, the use of different bottles, may be responsible for the non-linear behaviour of frequency percentiles concerning the percentage of adulteration, particularly noticeable in the 25th percentile for both adulterations. Although this fact presents clear challenges when drawing conclusions from the observed behaviour, it offers a clear advantage: the 75th percentile of frequency appears to be a more sensitive ultrasonic parameter than the other lower percentiles and velocity in distinguishing the predominant triglycerides present in the samples.

As can be seen, the results demonstrate that pure olive oil transmits lower frequency components compared to sunflower and corn oil, which are notably similar to each other. These findings align with previous studies [15], even though they were conducted using a 1 MHz frequency transducer, which also indicated a lower value of the frequency components transmitted by pure olive oil compared to sunflower and corn oils.

The analysis of adulterated olive oil samples reveals that once again, the frequency components are distributed among the extreme values of the pure samples, in the same order as the percentage of adulteration with sunflower or corn, though not precisely proportional. Moreover, an interesting observation is that the number of categories established in the classification decreases as higher frequency components are considered. This suggests that when studying the adulteration of olive oil with other oils, it is crucial to focus on the transmitted frequency components of lower value.

In the case of adulteration with sunflower oil, pure olive oil cannot be clearly distinguished until the mixture contains a proportion of sunflower greater than 40 %. This conclusion is based on the categorization established using the lower frequency components. On the other hand, when studying the adulteration of olive oil with corn oil, detection is possible with a corn proportion of 20 %. However, determining the precise percentage of corn adulteration becomes more challenging,

especially when attempting to do so based on the higher frequency components.

The similar behavior exhibited by the three shown frequency percentiles and the ultrasonic global loss is perfectly reflected when establishing a linear correlation among them. Thus, the mentioned equations for linear regression are shown in Equations (4), 5, and 6, including the regression coefficient R.

$$FFT25_l = (23600 \pm 1900)UGL + (240000 \pm 80000); R = 0.844 \quad (4)$$

$$FFT50_l = (16000 \pm 1300)UGL + (830000 \pm 50000); R = 0.842 \quad (5)$$

$$FFT75_l = (27600 \pm 2000)UGL + (700000 \pm 90000); R = 0.862 \quad (6)$$

As can be deduced, the more attenuating the sample is, the higher the frequency components of all percentiles become. Paradoxically, even though the signal is attenuated, there is a shift of the frequency components towards higher values. However, this shift is not identical for all percentiles. Thus, Eqs. (7), (8), and (9) show the existing linear relationships between the percentile differences and the ultrasonic global loss:

$$FFT50_l - FFT25_l = (-7600 \pm 800)UGL + (590000 \pm 40000); R = -0.753 \quad (7)$$

$$FFT70_l - FFT25_l = (4000 \pm 1200)UGL + (460000 \pm 50000); R = 0.384 \quad (8)$$

$$FFT75_l - FFT50_l = (11600 \pm 1200)UGL - (130000 \pm 50000); R = 0.779 \quad (9)$$

As an example, Fig. 8 graphically represents the linear correlation corresponding to equation (9). The results suggest that the distance between percentiles 75 and 50 increases with ultrasonic global loss, while the distance between percentiles 50 and 25 decreases. In other words, although all frequency components are attenuated, the higher frequencies are proportionally less affected.

4. Conclusions

The conducted studies confirm the suitability of ultrasonic inspection as a valid non-destructive method for the authentication and characterization of edible oil samples.

With regard to the propagation velocity of ultrasonic waves, the results indicate a linear decrease with temperature. The precise quantification of the corresponding fitting lines for both pure and mixed samples allows us to consider their dependence on the different composition, primarily the major triglycerides, present in the inspected oils. In general, the velocity values obtained in pure olive oil samples are clearly lower than those in pure corn oil, and the latter are lower than those in pure sunflower oil. In fact, in the prepared mixed samples, the slopes and intercepts of the regression lines corresponding to the mixture of olive oil with sunflower oil are higher than those with corn oil. Moreover, the determination of velocity at specific temperatures enables the estimation of the percentage presence of olive oil and sunflower/corn oil in the inspected mixed samples in several cases.

Regarding the ultrasonic global loss, its behaviour with temperature deviates from linearity. In this case, a maximum value is observed around 28–30 °C, which decreases to a greater or lesser extent as the temperature increases or decreases, depending on the considered sample. However, the evident fact that this behaviour is replicated in all samples, whether pure or mixed, emphasizes the influence that triglycerides have on ultrasonic global loss. In this case, not all triglycerides must exhibit the same dependence on ultrasonic global loss with temperature, as was the case with velocity, where they all decreased proportionally. Therefore, ultrasonic global loss is proposed as a more sensitive parameter for distinguishing the constituent

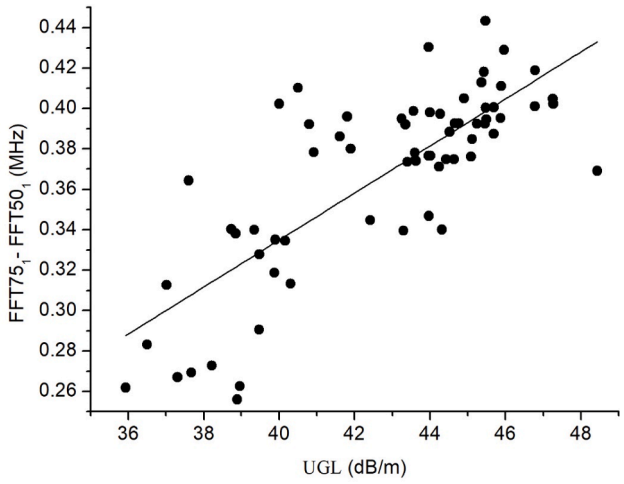

Fig. 8. Evolution of the frequency difference corresponding to percentiles 75 and 50 (FFT_{75}-FFT_{50}) versus the ultrasonic global loss of the samples and linear regression line between them.

triglycerides of a sample or, in other words, determining its fatty acid profile. Concerning pure samples, the lowest ultrasonic global loss values clearly correspond to olive oil, while the highest values are found in sunflower oil, although the latter shows similar values to corn oil.

Finally, the behaviour of the frequency percentiles with temperature is very similar to that of ultrasonic global loss. That is, there appears to be a maximum value for these percentiles around 30–32 °C, which then decreases as the temperature increases or decreases from that point. Once again, this behaviour is likely a consequence of the triglycerides present in the pure and mixed samples, suggesting that the frequency percentiles could serve as valid parameters to determine the triglyceride profile of a given sample. In this regard, since the errors associated with the 75th percentile are higher, it is generally more suitable for this purpose than the 25th or 50th percentiles. On the other hand, if the objective is to assess the potential adulteration of an olive oil sample, it is advisable to focus on the 25th percentile, which has lower errors. In this context, pure olive oil transmits significantly lower frequency components than sunflower and corn oil, which share similar characteristics.

As can be inferred, the results not only allow the characterization of pure and adulterated samples of edible oils but also open the possibility of determining the profile of fatty acids in a specific sample using the described ultrasonic parameters, with the added advantage of doing so non-destructively.

Declaration of competing interest

The authors declare that they have no known competing financial interests or personal relationships that could have appeared to influence the work reported in this paper.

Data availability

Data will be made available on request.

Appendix A. Supplementary data

Supplementary data to this article can be found online at https://doi.org/10.1016/j.ultras.2023.107216.

References

[1] M.R. Zarezadeh, M. Aboonajmi, M. Ghasemi-Varnamkhasti, Applications of ultrasound techniques in tandem with non-destructive approaches for the quality

evaluation of edible oils, J. Food Sci. Technol. 59 (2022) 2940–2950, https://doi.org/10.1007/s13197-022-05351-1.
[2] F. Gunstone, Vegetable oils in food technology: composition, properties and uses, John Wiley & Sons, 2011.
[3] M. Miller, N.J. Stone, C. Ballantyne, V. Bittner, M.H. Criqui, H.N. Ginsberg, A. C. Goldberg, W.J. Howard, M.S. Jacobson, P.M. Kris-Etherton, T.A. Lennie, M. Levi, T. Mazzone, S. Pennathur, Triglycerides and cardiovascular disease: A scientific statement from the American Heart Association, Circulation 123 (2011) 2292–2333, https://doi.org/10.1161/CIR.0b013e3182160726.
[4] D. Mozaffarian, T. Hao, E.B. Rimm, W.C. Willett, F.B. Hu, Changes in Diet and Lifestyle and Long-Term Weight Gain in Women and Men, N. Engl. J. Med. 364 (2011) 2392–2404, https://doi.org/10.1056/nejmoa1014296.
[5] K. Przykaza, H. Nikolaichuk, A. Kozub, J. Tomaszewska-Gras, Ž. Peršurić, S. K. Pavelić, E. Fornal, Newly marketed seed oils. What we can learn from the current status of authentication of edible oils, Food Control. 130 (2021), https://doi.org/10.1016/j.foodcont.2021.108349.
[6] A.M. Jergović, Ž. Peršurić, L. Saftić, S. Kraljević Pavelić, Evaluation of MALDI-TOF/MS Technology in Olive Oil Adulteration, JAOCS, J. Am. Oil Chem. Soc. 94 (2017) 749–757, https://doi.org/10.1007/s11746-017-2994-y.
[7] C. Jimenez-Lopez, M. Carpena, C. Lourenço-Lopes, M. Gallardo-Gomez, J. M. Lorenzo, F.J. Barba, M.A. Prieto, J. Simal-Gandara, Bioactive compounds and quality of extra virgin olive oil, Foods 9 (2020), https://doi.org/10.3390/foods9081014.
[8] A.G. Pereira, P. Otero, M. Fraga-Corral, P. Garcia-Oliveira, M. Carpena, M. A. Prieto, J. Simal-Gandara, State-of-the-art of analytical techniques to determine food fraud in olive oils, Foods 10 (2021) 1–24, https://doi.org/10.3390/foods10030484.
[9] M.R. Zarezadeh, M. Aboonajmi, M. Ghasemi Varnamkhasti, Fraud detection and quality assessment of olive oil using ultrasound, Food Sci. Nutr. 9 (2021) 180–189, https://doi.org/10.1002/fsn3.1980.
[10] M.R. Zarezadeh, M. Aboonajmi, M.G. Varnamkhasti, F. Azarikia, Olive Oil Classification and Fraud Detection Using E-Nose and Ultrasonic System, Food Anal. Methods 14 (2021) 2199–2210, https://doi.org/10.1007/s12161-021-02035-y.
[11] J. Yan, W.M.D. Wright, J.A. O'Mahony, Y. Roos, E. Cuijpers, S.M. van Ruth, A sound approach: Exploring a rapid and non-destructive ultrasonic pulse echo system for vegetable oils characterization, Food Res. Int. 125 (2019), 108552, https://doi.org/10.1016/j.foodres.2019.108552.
[12] B. Alouache, D. Laux, A. Hamitouche, K. Bachari, T. Boutkedjirt, Ultrasonic characterization of edible oils using a generalized fractional model, Appl. Acoust. 131 (2018) 70–78, https://doi.org/10.1016/j.apacoust.2017.10.014.
[13] S. Ghosh, M. Holmes, M. Povey, Temperature Dependence of Bulk Viscosity in Edible Oils using Acoustic Spectroscopy, J. Food Process. Technol. 08 (2017), https://doi.org/10.4172/2157-7110.1000676.
[14] N.A. Azman, S.B. Abd Hamid, Determining the Time of Flight and Speed of Sound on Different types of Edible Oil, IOP Conf, Ser. Mater. Sci. Eng. (260 2017.), https://doi.org/10.1088/1757-899X/260/1/012034.
[15] A. Jiménez, M. Rufo, J. Paniagua, A. González-Mohino, L.S. Olegario, New findings of edible oil characterization by ultrasonic parameters, Food Chem. 374 (2022), 131721, https://doi.org/10.1016/j.foodchem.2021.131721.
[16] A. Jiménez, M. Rufo, J.M. Paniagua, A. González-Mohino, L.S. Olegario, Authentication of pure and adulterated edible oils using non-destructive ultrasound, Food Chem. 429 (2023), 136820, https://doi.org/10.1016/j.foodchem.2023.136820.
[17] M.S. Rashed, J. Felfoldi, Ultrasonic method for identifying oil types and their mixtures, Prog. Agric. Eng. Sci. 14 (2018) 111–119, https://doi.org/10.1556/446.14.2018.S1.11.
[18] R.M. Baêsso, P.A. Oliveira, G.C. Morais, A.V. Alvarenga, R.P.B. Costa-Félix, Use of ultrasound to monitor physical properties of soybean oil, J. Phys. Conf. Ser. 733 (2016), https://doi.org/10.1088/1742-6596/733/1/012042.
[19] S.K.M. Ali, B. Ali, Acoustics Impedance Studies in Some Commonly Used Edible Oils, 1 (2014) 563–566.
[20] H. Qi, J. Ba, J.M. Carcione, L. Zhang, Temperature-Dependent Wave Velocities of Heavy Oil-Saturated Rocks, Lithosphere. 2022 (2022), https://doi.org/10.2113/2022/3018678.
[21] H. Qi, J. Ba, T.M. Müller, Temperature Effect on the Velocity-Porosity Relationship in Rocks, J. Geophys. Res. Solid Earth. 126 (2021) 1–23, https://doi.org/10.1029/2019JB019317.
[22] L.E. Kinsler, A.R. Frey, A.B. Coppens, J. V Sanders, Fundamentals of acoustics, Fundam. Acoust. 4th Ed. by Lawrence E. Kinsler, Austin R. Frey, Alan B. Coppens, James V. Sanders, pp. 560. ISBN 0-471-84789-5. Wiley-VCH, December 1999. 1 (1999) 560, doi:10.1002/9780470612439.
[23] Z. Maekawa, Environmental and architectural acoustics, CRC Press, 1993.
[24] A. Jiménez, M. Rufo, J.M. Paniagua, A.T. Crespo, M.P. Guerrero, M.J. Riballo, Contributions to ultrasound monitoring of the process of milk curdling, Ultrasonics. 76 (2017) 192–199, https://doi.org/10.1016/j.ultras.2017.01.007.
[25] A. González-Mohino, A. Jiménez, M.J. Paniagua, T. Perez-Palacios, M. Rufo, New contributions of ultrasound inspection to the characterization of different varieties of honey, Ultrasonics (2019), https://doi.org/10.1016/j.ultras.2019.02.010.
[26] M.P. Norton, D.G. Karczub, Fundamentals of noise and vibration analysis for engineers, Cambridge University Press, 2003.
[27] T. Gudra, K.J. Opielinski, Applying spectrum analysis and cepstrum analysis to examine the cavitation threshold in water and in salt solution, Ultrasonics 42 (2004) 621–627, https://doi.org/10.1016/j.ultras.2003.11.016.
[28] V.A. Del Grosso, C.W. Mader, Speed of sound in pure water, J. Acoust. Soc. Am. 52 (1972) 1442–1446.
[29] H. Bunjes, M.H.J. Koch, K. Westesen, Effect of particle size on colloidal solid triglycerides, Langmuir 16 (2000) 5234–5241, https://doi.org/10.1021/la990856l.
[30] A.B. Koc, B. Ozer, Nondestructive monitoring of renetted whole milk during cheese manufacturing, Food Res. Int. 41 (2008) 745–750, https://doi.org/10.1016/j.foodres.2008.05.008.
[31] A. González-Mohino, A. Jiménez, M. Rufo, J.M. Paniagua, L.S. Olegario, S. Ventanas, Correlation analysis between acoustic and sensory technique data for cooked pork loin samples, LWT 141 (2021), 110882.
[32] X. Zhong, D. Zhang, Latency prediction of earmuff using a lumped parameter model, Appl. Acoust. 176 (2021), 107870, https://doi.org/10.1016/j.apacoust.2020.107870.
[33] S. Rubalya Valantina, R. Chandiramouli, P. Neelamegam, Detection of adulteration in olive oil using rheological and ultrasonic parameters, Int. Food Res. J. 20 (2013) 3197–3202.
[34] A. Ratajski, I. Białobrzewski, F. Dajnowiec, S. Bakier, The Use of Ultrasonic Methods in the Identification of Honey Types, Tech. Sci. 13 (2010) 22–29.
[35] M. Oroian, Measurement, prediction and correlation of density, viscosity, surface tension and ultrasonic velocity of different honey types at different temperatures, J. Food Eng. 119 (2013) 167–172, https://doi.org/10.1016/j.jfoodeng.2013.05.029.
[36] Z. Wang, A. Nur, Effect of temperature on wave velocities in sands and sandstones with heavy hydrocarbons, SPE Reserv. Eng. 3 (1988) 158–164.
[37] R. Punturo, H. Kern, R. Cirrincione, P. Mazzoleni, A. Pezzino, P- and S-wave velocities and densities in silicate and calcite rocks from the Peloritani Mountains, Sicily (Italy): The effect of pressure, temperature and the direction of wave propagation, Tectonophysics. 409 (2005) 55–72, https://doi.org/10.1016/j.tecto.2005.08.006.
[38] W. Chaiyasit, R.J. Elias, D.J. McClements, E.A. Decker, Role of physical structures in bulk oils on lipid oxidation, Crit. Rev. Food Sci. Nutr. 47 (2007) 299–317, https://doi.org/10.1080/10408390600754248.
[39] B. Gao, Y. Luo, W. Lu, J. Liu, Y. Zhang, L. (Lucy) Yu, Triacylglycerol compositions of sunflower, corn and soybean oils examined with supercritical CO2 ultra-performance convergence chromatography combined with quadrupole time-of-flight mass spectrometry, Food Chem. 218 (2017) 569–574, https://doi.org/10.1016/j.foodchem.2016.09.099.
[40] S.M. Ghazani, A.G. Marangoni, Healthy Fats and Oils, second ed., Elsevier Ltd. (2016). doi: 10.1016/b978-0-08-100596-5.00100-1.
[41] S.K. Lo, C.P. Tan, K. Long, M.S.A. Yusoff, O.M. Lai, Diacylglycerol oil-properties, processes and products: A review, Food Bioprocess Technol. 1 (2008) 223–233, https://doi.org/10.1007/s11947-007-0049-3.
[42] H. Yanai, Y. Tomono, K. Ito, N. Furutani, H. Yoshida, N. Tada, Diacylglycerol oil for the metabolic syndrome, Nutr. J. 6 (2007) 1–6, https://doi.org/10.1186/1475-2891-6-43.
[43] B.M. McKenna, Texture in food: Semi-solid foods, Woodhead Publishing, 2003.
[44] J. Orsavova, L. Misurcova, J. Vavra Ambrozova, R. Vicha, J. Mlcek, Fatty acids composition of vegetable oils and its contribution to dietary energy intake and dependence of cardiovascular mortality on dietary intake of fatty acids, Int. J. Mol. Sci. 16 (2015) 12871–12890, https://doi.org/10.3390/ijms160612871.
[45] D.L. Katz, K. Doughty, A. Ali, Cocoa and chocolate in human health and disease, Antioxidants Redox Signal. 15 (2011) 2779–2811, https://doi.org/10.1089/ars.2010.3697.